Optical and Quantum Electronics **26** *(1994) S547–S557*

Tuneable fibre source for picosecond pulses around 1.55 μm with repetition rates up to 20 GHz

TH. PFEIFFER, G. VEITH
Alcatel SEL Research Centre, 70430 Stuttgart, Germany

Received 9 July; revised 11 August; accepted 1 September 1993

We report on the generation of picosecond optical pulses around 1.55 μm using a tuneable actively mode-locked erbium-doped fibre ring laser. Pulse widths of less than 10 ps have been achieved within the wavelength range 1518 to 1570 nm at a pulse repetition rate of 20 GHz. Pulse trains with lower repetition rates have been generated using electrical square-wave signals for driving the electrooptic modulator, resulting in <20 ps pulse widths. The implementation of an all polarization-preserving fibre ring cavity enabled stable and reproducible operation of the laser. Minimization of the overall ring dispersion offers tuneability at nearly constant repetition rate throughout the whole wavelength range. Simple analytic expressions are given that allow for optimization of the ring laser performance with respect to output power, relaxation oscillations and wavelength tuneability at constant repetition rate.

1. Introduction

Erbium-doped fibre lasers (EFRL) have attracted increasing interest during recent years because of attractive features such as <10 kHz linewidth in single-line continuous-wave (cw) operation [1] or picosecond [2] and femtosecond [3] pulse generation at multigigahertz repetition rates [4]. All these properties, as well as the output power, can be made constant through the whole wavelength tuning range of the laser. The tuning range is compatible with the gain bandwidth of erbium-doped fibre amplifiers (EDFA), which makes these lasers specially attractive for use in future optical telecommunication systems at 1.55 μm. The development of the EFRL has profited by the rapid development of EDFA technology in the past. There are many possible applications of pulsed EFRL in telecommunication systems. They can be used as a master source of high-repetition-rate bandwidth-limited picosecond optical pulses for signal transmission and for all-optical signal processing such as signal regeneration and all-optical switching. High-repetition-rate lasers can be used, for example, as clock sources in an all-optical repeaters for digital transmission. For all-optical demultiplexing of optical time-division multiplexed (OTDM) signals, picosecond-pulse lasers with lower repetition rates are needed. Finally, the provision of a tuneable source for picosecond pulse propagation studies in the 1.55-μm transmission window should be mentioned.

In this paper we present an actively amplitude-modulated (AM) mode-locked erbium-doped fibre ring laser. It was developed as a source of widely tuneable picosecond pulses at variable

0306–8919

repetition rates up to 20 GHz for use in digital transmission systems and for measurement purposes. After the presentation of our experimental equipment we first discuss some measurements showing the general output power characteristics of the EFRL. Picosecond pulses have been generated at megahertz and multigigahertz repetition rates. Both issues are addressed in separation sections.

2. Experimental set-up

Figure 1 shows the basic laser configuration used in the experiments presented in this paper. In the experiments with continuous wave (cw) operation and low-repetition-rate pulse generation described in the next two sections, some of the components were made of standard non-polarization-preserving fibres, so manual polarization controllers had to be included. The latest version of the ring laser cavity used for multigigahertz pulse generation consists of all polarization-preserving fibre components. The erbium-doped fibre is pumped (point 2 in Fig. 1) by 70 mW at 980 nm via a wavelength-dependent fused-fibre coupler. The doped fibre itself is 20.8 m long and provides a saturated signal output power of +12.7 dBm (point 1 in Fig. 1) at 1549 nm for the pump power stated above. The laser cavity includes a polarization-sensitive optical isolator to accomplish travelling-wave operation. Part of the circulating optical power is extracted by an asymmetric output coupler that reflects 80% at 1550 nm into the ring. The AM modulation is induced by an electrooptic Mach–Zehnder type amplitude modulator. Its optical 3-dB bandwidth is specified at 11 GHz, the switching voltage is $U_\pi = 4.1$ V. The electrical driving signal applied to the modulator was a sinewave for 20 GHz pulse repetition rate and a quasi-square-wave signal at megahertz repetition rates. Details are given with the corresponding measurements below. Wavelength tuning of the laser is performed by an angle-tuned etalon filter with a 3-dB bandwidth of 3.5 nm at 1520 nm and 2.5 nm at 1567 nm. The ring loss was measured before closing the ring using a polarized semiconductor test laser at 1549 nm. The overall loss was measured as −9.7 dB from point 1 to point 2 in Fig. 1. The polarization extinction was better than 20 dB. The excess loss from point 1 to the output port of the ring was about −3 dB, including the coupler, isolator and splice losses.

The laser emission was analysed using different measuring equipment. The pulses were analysed using a streak camera with a specified resolution of 4.5 ps full-width at half-maximum (FWHM) at a streak repetition rate of 140 MHz. Alternatively, a 40-GHz PIN photodiode/50-GHz sampling oscilloscope set-up was used giving a theoretical temporal resolution of

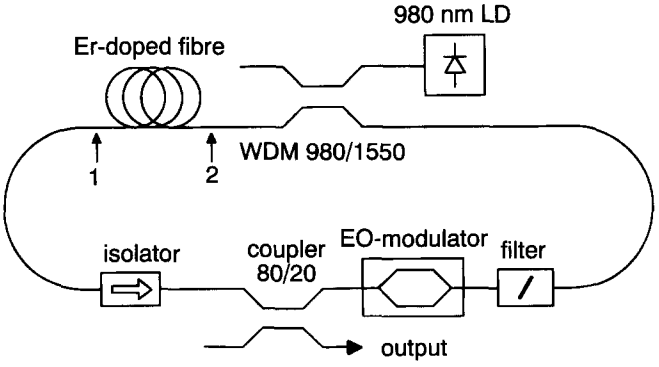

Figure 1 Set-up of tuneable actively mode-locked erbium-doped fibre ring laser. It consists of all polarization-preserving fibres, including the erbium-doped fibre.

12.8 ps FWHM. The mode-locking quality of the low-frequency pulse trains was also analysed using a 10-GHz PIN photodiode with a 21-GHz electrical spectrum analyser. The optical spectrum was measured using a double-stage grating monochromator with a wavelength resolution of 0.1 nm and dynamic range of 55 dB at 1 nm beside the optical carrier.

3. CW measurements

In this section we present some results showing the output power characteristics of the CW-operated ring laser. They were achieved with an earlier ring laser set-up, consisting of mainly standard fibre components. The technical data differ in some details from those given in the previous section and are given in the literature cited below. The general features of the output power also apply to the case of mode-locked operation. For picosecond pulses at repetition rates above 1 MHz, the gain of the erbium-doped fibre is the same as in the case of a CW signal, provided the average power is the same in both cases.

Figure 2 shows the emission spectrum of the ring laser at wavelengths between 1520 and 1570 nm. As can be seen, the output power of +8.5 dBm is nearly constant within the whole tuning range. The active fibre has been chosen long enough for large small-signal gain and is operated deep in saturation. Then, if the pump power is well above threshold, the ring laser output power P_{laser} is approximately independent of the emission wavelength λ_L as expressed by [5]

$$P_{\text{laser}} = \frac{\lambda_p}{\lambda_L} \frac{V_1(1-R)}{1-G_0^{-1}} \cdot P_{\text{pump}} \tag{1}$$

Here the pump power P_{pump} (at point 2 in Fig. 1) is supplied at wavelength λ_p; the transmission factor from point 1 in Fig. 1 to the output port of the laser is described by $V_1(1-R)$; the steady state ring gain G_0 is given by the ring losses V and the reflection R of the output coupler as $G_0 = 1/(VR)$. If the transmission factors of the intracavity components are independent of wavelength, then the output power is constant, except for the small variation (3.2%) inferred from λ_L in the denominator of Equation 1. Equation 1 implies that the erbium-doped fibre is operating as a power amplifier, converting each pump photon into one laser photon. This approximation is valid, as long as the small-signal gain of the fibre is large compared to the ring gain G_0 and the pump power is well above the threshold power. A more detailed analysis is given in [5], which also describes more general situations such as operation near threshold or unsaturated fibre gain. This theoretical analysis can be used for optimizing the ring cavity

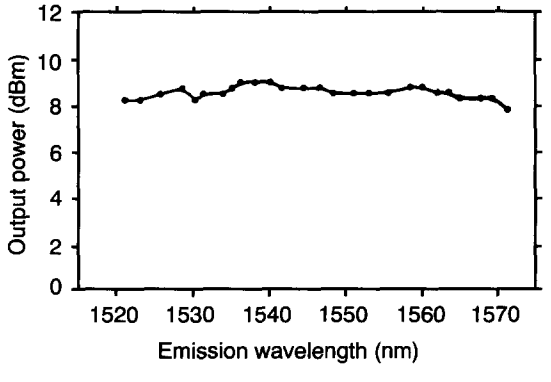

Figure 2 Power tuning curve of cw-operated EFRL. Pump power is 52 mW at 980 nm, output coupler reflection $R = 42\%$.

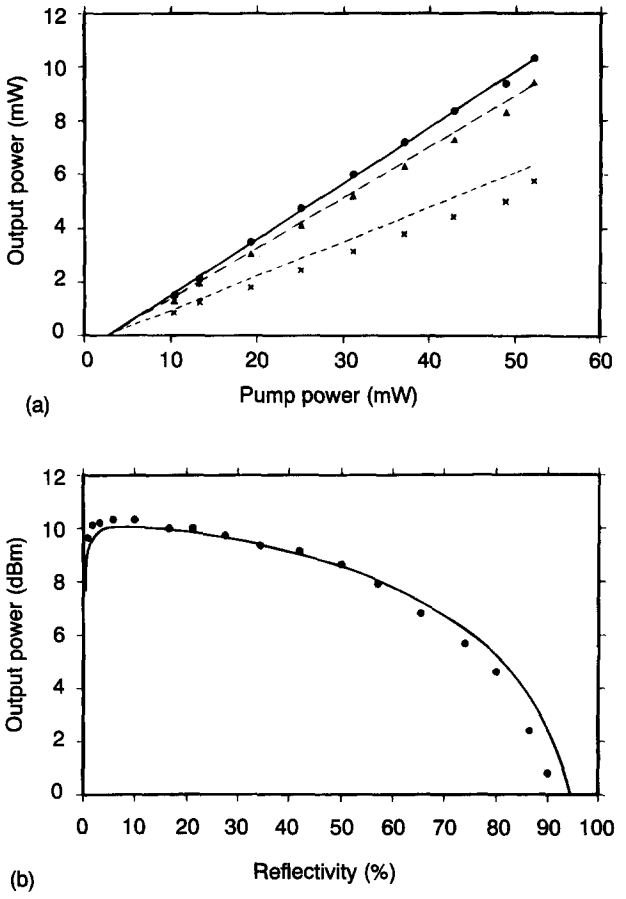

Figure 3 (a): Output power of cw-operated EFRL as a function of pump power for different reflection factors at the output. ●: $R = 10\%$; ▲: $R = 27\%$; x: $R = 57\%$. (b): Output power as a function of output coupler reflectivity for 52 mW pump power. $L = 20$ m. Emission wavelength is 1533 nm in both cases.

design with respect to the average output power under different operating conditions [5, 6]. Figure 3 gives an example of how the output power varies with pump power for different reflection factors and with reflection factor at constant pump power. The points are experimental values, the solid lines are theoretical calculations using the full analysis [5]. As can be seen from the diagram, there is an optimum of the reflection factor near $R = 5\%$ to 10%, yielding an output power of 10 mW. However, this low reflection greatly reduces the tuning range of the EFRL and increases the instability of the laser emission. For larger tuning range and greater stability, the output coupler should reflect more than 40% of the circulating power into the ring.

In Fig. 4 the dependence of the relaxation oscillation frequency and linewidth on the laser output power is shown for an emission wavelength of 1550 nm. Also included is the r.m.s. amplitude of the relaxation oscillation. The relaxation frequency is <35 kHz, varying as the square root of the output power [7]. The linewidth is <3.2 kHz, varying linearly with the output power at higher powers. The amplitude is about constant at 4.5 μW, corresponding to <1% of the output power. An extended time-dependent version of the above analysis [8] describes the properties of the relaxation oscillations as a function of the laser power, the pump power

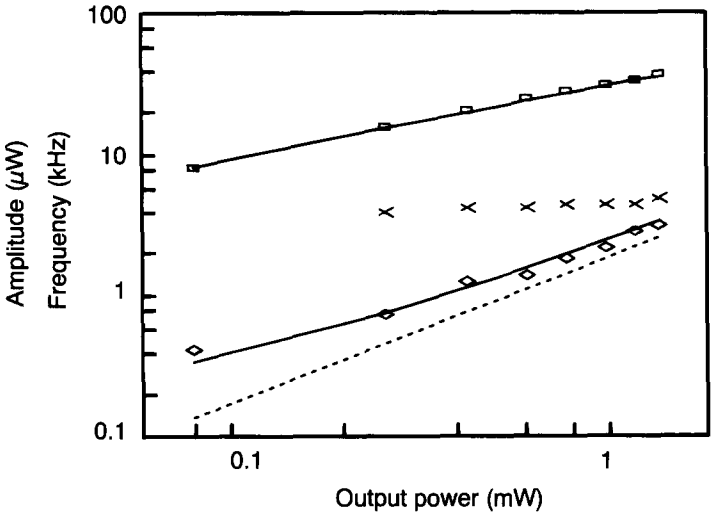

Figure 4 Measured dependence of relaxation oscillation frequency (□), damping constant (◇) and amplitude (×) on laser output power at emission wavelength 1550 nm. Solid lines are calculated using Equations 2 and 3. Dashed line is a linear approximation of the linewidth versus output power dependence. $\lambda = 1550$ nm.

and emission wavelength:

$$\omega_0^2 = \frac{1 - G_0^{-1}}{\tau T} \frac{P_L^{\text{out}}}{P_L^{\text{sat}}} \tag{2}$$

$$\omega_d = \frac{1}{2\tau} \left\{ \frac{P_p^{\text{out}}}{P_p^{\text{sat}}} + \frac{P_L^{\text{out}}}{P_L^{\text{sat}}} + 1 \right\} \tag{3}$$

where $\omega_0/2\pi$ is the relaxation frequency, ω_d/π is the electrical 3 dB linewidth (ω_d = damping constant), T is the cavity round-trip time and $\tau = 10$ ms is the upper-level spontaneous lifetime of the erbium ions. P_p^{out} and P_L^{out} are the output pump power and laser power as measured at the output end of the active fibre. P_L^{out} is related to the EFRL output power by $P_L^{\text{out}} = P_{\text{laser}}/V_1(1-R)$. P_p^{sat} and P_L^{sat} are the corresponding saturation powers as given in [5]. They describe the dependence of the relaxation oscillation properties on emission and pump wavelength. It is found experimentally that for 1 mW EFRL output power the oscillation frequency is in the range 20 to 60 kHz, the linewidth 2 to 6 kHz and the amplitude 3 to 6 μW within the whole tuning range of 1520 to 1570 nm.

4. Low-repetition-rate pulse generation

In this section we present the generation of picosecond pulses with repetition rates of several hundred megahertz. These low repetition rates are used for switching applications such as time domain demultiplexing of OTDM signals and for measuring purposes such as pulse propagation and dispersion measurements. Moreover, the greater ease of measurement gives some useful insight into the mode-locked ring laser operation.

The EFRL is mode-locked by driving the electrooptic modulator with a periodic electric driving signal. In our case the modulator is operated about the point of its maximum transmission, so the resulting pulse repetition frequency f_{rep} is twice the modulation frequency f_{mod}. The generation of short optical pulses requires an electrical driving signal with steep

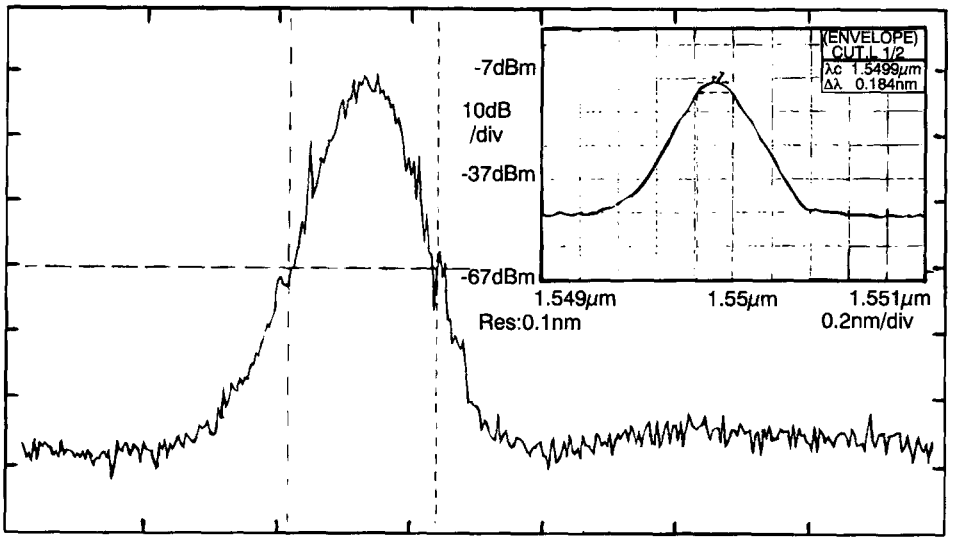

Figure 5 Optical pulse of mode-locked EFRL at 1550 nm with 464 MHz repetition rate measured with a 40-GHz PIN photodiode/50-GHz sampling oscilloscope (timescale 20 ps/div). The corresponding optical spectrum is shown in the inset. Deconvolved pulse width is 18.4 ps; spectral width is 0.18 nm.

slopes in order to shorten the temporal gate width of the electrooptic modulator. For a sine-wave driving signal the resulting optical pulse width generated by the EFRL varies with the modulation frequency as [9] FWHM $\propto 1/\sqrt{f_{\text{mod}}}$. For low modulation frequencies in the range of 100 MHz this would result in optical pulse widths in the order of >100 ps for the laser configuration used in our experiments. Shorter pulses are achieved when a square-wave driving signal is applied to the modulator. In Fig. 5 an output pulse is shown that was generated at a repetition frequency of 464 MHz at 1550 nm. The driving signal was square-wave-shaped at 232 MHz with rise/fall time of 100/300 ps. The modulation index of the electrooptic modulator was $m = 50\%$. The optical pulse width was measured using a fast PIN photodiode/sampling oscilloscope set-up (temporal resolution 21.8 ps) and was $\Delta\tau = 18.4$ ps after deconvolution. The optical spectrum is shown in the inset. The 3-dB bandwidth is $\Delta\lambda = 0.18$ nm (corresponding to $\Delta f = 22.5$ GHz), resulting in a time–bandwidth product (TBP) of $\Delta\tau\,\Delta f = 0.414$. This is close to the theoretical limit for Fourier-transform-limited Gaussian pulses ($\Delta\tau\,\Delta f = 0.441$). The small ringing that can be seen on the trailing edge of the pulse is due to the limited time response of the measuring equipment. The shape of the optical spectrum is smooth, showing no spurious wavelength components up to 40 dB below the centre wavelength, indicating that the active fibre is operating in deep saturation. Information about the quality of the mode-locking operation is obtained from the electrical spectra in Fig. 6 (pulse repetition rate 133 MHz). They have been measured using a 10-GHz photodiode and a 21-GHz electrical spectrum analyser. In the upper diagram, depicting the frequency range 0 to 1.8 GHz, sharp lines at frequencies equal to integer multiples of the pulse repetition frequency are to be seen. The free spectral range of the ring laser cavity is given by the round-trip frequency as FSR = 4.76 MHz. For a pulse repetition rate of 133 MHz this means that only every 28th longitudinal cavity mode is oscillating. Short-term pulse-to-pulse fluctuations of amplitude and timing would give rise to additional frequency components between two neighbouring harmonics. The absence of these frequency components within >40 dB below

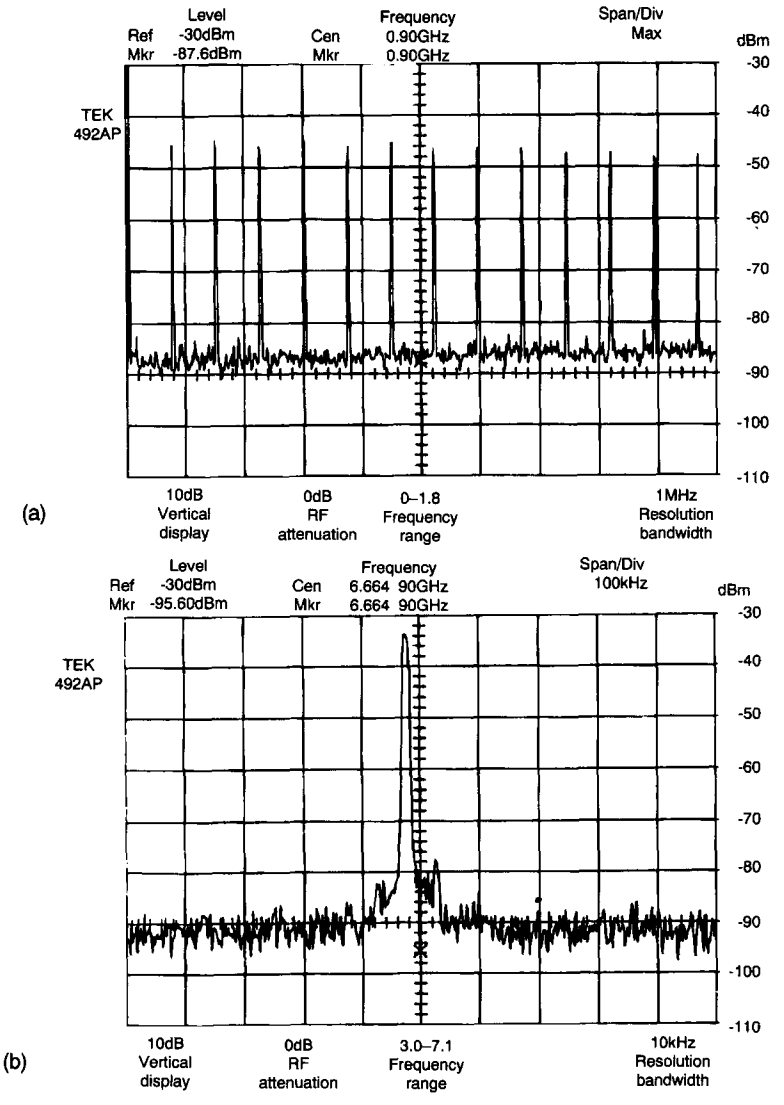

Figure 6 Electrical spectrum of 133 MHz pulse train. (a): First 13 harmonics (0 to 1.8 GHz). (b): 50th harmonic at 6.66 GHz (1 MHz span).

the carriers is a measure of the stability of the pulses on a timescale comparable to the inverse repetition rate. Amplitude and timing jitter of the optical pulses on a longer timescale would show up in the electrical spectrum at higher harmonics of the pulse repetition rate [10]. The lower part of Fig. 6 shows a 1-MHz sweep around 6.66 GHz, corresponding to the 50th harmonic of the pulse repetition rate. The better resolution of 10 kHz reveals that within nearly 60 dB below the carrier there are no frequency components beside the carrier. The only frequency detected is due to the relaxation oscillation at 60 kHz with an amplitude of 48 dB below the carrier (electrical). Thus, according to the analysis presented in [10] the r.m.s. timing jitter in this experiment is <1 ps.

While tuning the EFRL emission wavelength, the modulation frequency had to be changed

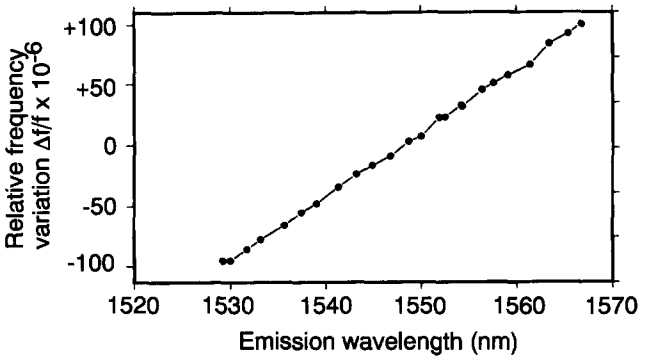

Figure 7 Dependence of pulse repetition frequency on laser emission wavelength for good-quality mode-locking. Zero on the vertical scale corresponds to 133.295 MHz. –●– Repetition frequency, MHz.

owing to the wavelength-dependent round-trip time. Figure 7 shows the wavelength-dependent pulse reception rate $f_{\text{rep}} = 2f_{\text{mod}}$. A linear regression to the experimental data yields $(1/f_{\text{rep}})\mathrm{d}f_{\text{rep}}/\mathrm{d}\lambda = +5.5 \times 10^{-6}\,\text{nm}^{-1}$ relative change of the repetition frequency with wavelength. The relative change in repetition frequency is given approximately by

$$\frac{1}{f_{\text{rep}}}\frac{\mathrm{d}f_{\text{rep}}}{\mathrm{d}\lambda} = -c\frac{\sum_i D_i L_i}{\sum_i n_i^{\text{gr}} L_i} \tag{4}$$

with the vacuum speed of light c, group velocity dispersion D_i (usually given in $\text{ps nm}^{-1}\,\text{km}^{-1}$) and group velocity index n_i^{gr} for the fibre segment number i with length L_i. Setting $n_i^{\text{gr}} = 1.47$ and $D = +16\,\text{ps nm}^{-1}\,\text{km}^{-1}$ for the undoped fibre pigtails [11] (total length 13 m) and $D = -50\,\text{ps nm}^{-1}\,\text{km}^{-1}$ for the doped fibre [11] (length 30 m), the calculated value is $(1/f_{\text{rep}})\mathrm{d}f_{\text{rep}}/\mathrm{d}\lambda = +6.1 \times 10^{-6}\,\text{nm}^{-1}$, in good agreement with the measured value.

5. 20-GHz pulse generation

Optical pulses with repetition rates of 20 GHz have been generated by driving the amplitude modulator with an electrical sine-wave at 10 GHz. The amplitude of the modulation signal was $U_{\text{peak}} = U_\pi$, resulting in 100% modulation depth. The optical pulses were analysed using a streak camera system with temporal resolution of 4.5 ps FWHM. For this purpose the pulse repetition rate had to be adjusted at an exact integer multiple of the streak frequency, which had to be in the range 140 ± 0.250 MHz. On the other hand, the repetition rate was also an integer multiple of the ring free spectral range (6.4 MHz in this configuration). The measured pulse train at 1560 nm and the corresponding optical spectrum are shown in Fig. 8. The displayed pulse width is 10 ps. Taking into account the resolution of the streak camera (4.5 ps), the optical pulse width is 8.9 ps. The residual amplitude fluctuation of the pulses is due to nonstabilized operation of the EFRL. The optical spectrum shown in Fig. 8 is well approximated by a parabola on a logarithmic scale, which is related to Gaussian shaped pulses. The bandwidth of the spectrum is $\Delta\lambda = 0.54$ nm, corresponding to $\Delta f = 66.5$ GHz. Assuming transform-limited Gaussian pulses with $\Delta\tau\Delta f = 0.441$, the expected pulse width would be $\Delta\tau = 6.6$ ps. The longer pulse width measured with the streak camera is supposed to be due to timing jitter of the pulses. Since the measuring time interval of the camera is 1 s, timing fluctuations of the optical pulses relative to the electrical trigger of the streak camera accumulate to a broadened

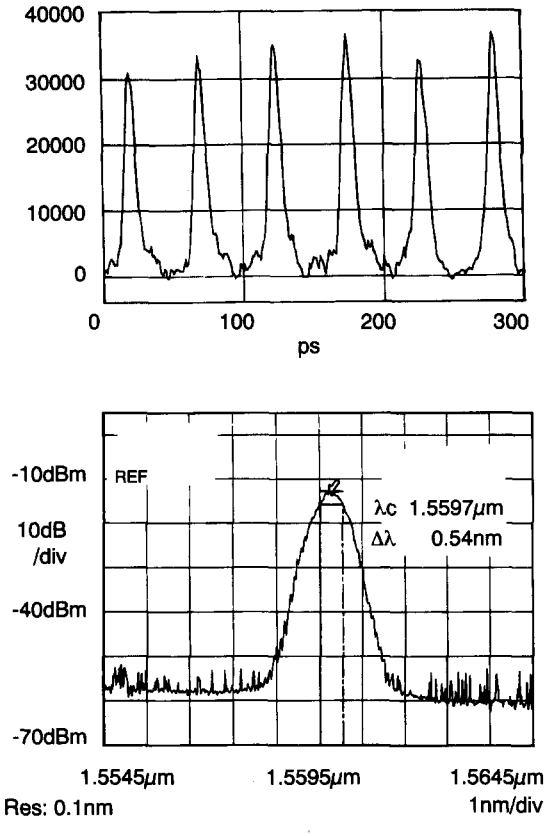

Figure 8 Streak camera measurement of 20-GHz pulse train at 1560 nm; displayed pulse width is 10 ps. The corresponding optical spectrum is shown in the lower diagram.

pulse. A comparison of the measured and calculated pulse widths implies an r.m.s. timing jitter of 6.0 ps, if the jitter is assumed to be Gaussian distributed. This value may be explained in part by the fact that the ring laser cavity incorporates about 32 m of optical fibre. The cavity length was not stabilized in these experiments, so temperature variations as well as mechanical vibrations can lead to phase fluctuations of the pulse train. In addition, the operating point of

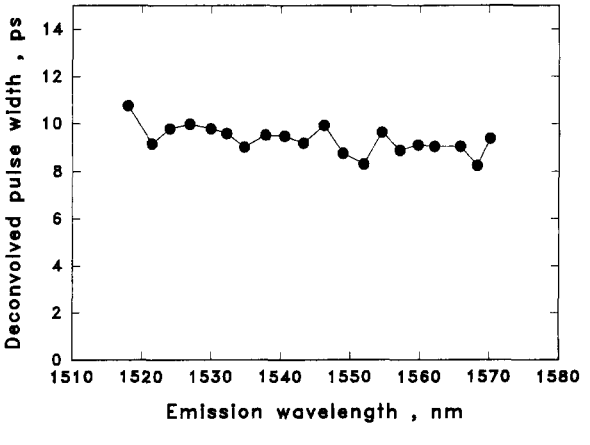

Figure 9 Deconvolved pulse width as measured with the streak camera (4.5 ps resolution) as function of emission wavelength. Pulse repetition rate is 20 GHz.

the amplitude modulator was not stabilized either. So a drift of the bias point is converted into timing fluctuations as well. A more reliable measurement of the pulse width is expected from nonlinear autocorrelation measurements [12], which are inherently insensitive to timing jitter.

20-GHz pulses such as those shown in Fig. 8 have been generated within the whole tuning range of 1518 to 1570 nm (Fig. 9). The measured pulse width is almost constant in this wavelength range. The modulation frequency (10 GHz) had to be changed by 430 kHz while tuning the laser over 52 nm, corresponding to a relative frequency change of $(1/f_{\mathrm{mod}})\mathrm{d}f_{\mathrm{mod}}/\mathrm{d}\lambda = +8.2 \times 10^{-7}\,\mathrm{nm}^{-1}$. This value is almost an order of magnitude lower than that measured with the configuration described in the previous section owing to the different fibre dispersion used in this set-up. It shows that it is possible to design a cavity with almost zero overall ring dispersion that is needed for constant-repetition-rate operation of the EFRL.

In a recent measurement the repetition rate of the mode-locked pulses was extended to 40 GHz within the tuning range of 1522 to 1565 nm [13]. This is the highest repetition rate reported so far for actively mode-locked fibre lasers, especially in connection with a large wavelength tuning range. The deconvolved pulse width was <6 ps FWHM in this experiment.

6. Conclusion

We have shown that with the mode-locked EFRL, tuneable picosecond pulses at multigigahertz repetition rates can be generated with properties that make the device attractive for application in high-speed optical transmission systems at 1.55 μm. These properties are picosecond duration (<10 ps) at quasi-continuously variable repetition rate up to 40 GHz; tuneability in a wide wavelength range (>40 nm); and narrow spectral width, close to the theoretical limit for transform-limited Gaussian pulses. For practical applications there remain, however, some points to be considered.

The relative stabilization of the modulation frequency and the pulse round-trip frequency is essential for the generation of stable pulses. During the experiments it was observed that the modulation frequency had to be within $<10^{-6}$ of the ideal value to generate stable pulses. This implies good thermal isolation of the ring cavity and some control circuit for readjustment of either the modulation frequency or the cavity length. The latter can be done [14] by mechanically stretching a part of the ring fibre using a phase-locked loop for control. The variation of the pulse repetition frequency while tuning the emission wavelength can be minimized by careful design of the laser cavity dispersion as described by Equation 4.

Acknowledgement

This work was partly supported by the European Community under the RACE ARTEMIS (R2015) contract. The polarization-preserving erbium-doped fibres were supplied by the contract partners Pirelli and University of Southampton. The dispersion measurements on the erbium-doped fibres and on the undoped fibres were performed by B. Deutsch at the University of Kaiserslautern.

References

1. H. SCHMUCK, Th. PFEIFFER and G. VEITH, *Electron. Lett.* **27** (1991) 2117.
2. Th. PFEIFFER and H. SCHMUCK, *2nd Topical Meeting on Optical Amplifiers and their Applications*, Snowmass Village *Techn. Digest* **13** (1991) 116.
3. D. J. RICHARDSON, A. B. GRUDININ and D. N. PAYNE, *Electron. Lett.* **28** (1992) 778.
4. A. TAKADA and H. MIYAZAWA, *Electron. Lett.* **26** (1990) 216.
5. Th. PFEIFFER, H. SCHMUCK and H. BÜLOW, *Photon. Technol. Lett.* **4** (1992) 847.

6. H. SCHMUCK, Th. PFEIFFER and H. BÜLOW, *Electron. Lett.* **28** (1992) 1637.
7. A. YARIV, *Quantum Electronics* (Wiley, New York, 1989).
8. Th. PFEIFFER, to be published.
9. D. J. KUIZENGA and A. E. SIEGMAN, *IEEE J. Quantum Electron.* **QE-6** (1970) 694.
10. J. KLUGE, D. WIECHERT and D. VON DER LINDE, *Optics Commun.* **51** (1984) 271.
11. B. DEUTSCH and Th. PFEIFFER, *Electron. Lett.* **28** (1992) 303.
12. See, e.g., *Ultrashort Light Pulses*, edited by S. L. Shapiro (Springer-Verlag, Berlin, 1977).
13. Th. PFEIFFER and G. VEITH, *Electron. Lett.* **29** (1993) 1849.
14. X. SHAN, D. CLELAND and A. ELLIS, *Electron. Lett.* **28** (1992) 182.